

New uranium-lead zircon dates from the Lynn Lake greenstone belt, northwestern Manitoba (part of NTS 64C14): implications for diverse granitoid magmatism and gold mineralization

by X.M. Yang

In Brief:

- Two new precise U-Pb zircon dates establish the timing of syn- to post-Sickle granitoid intrusions, each with distinct geochemical traits
- The Motriuk Lake quartz diorite shows an adakitic signature, while the Little Brightsand Lake leucogranite is highly fractionated
- Syn- to post-Sickle adakitic granitoids reflect post-arc magmatism and track gold mineralization

Citation:

Yang, X.M. 2024: New uranium-lead zircon dates from the Lynn Lake greenstone belt, northwestern Manitoba (part of NTS 64C14): implications for diverse granitoid magmatism and gold mineralization; *in* Report of Activities 2024, Manitoba Economic Development, Investment, Trade and Natural Resources, Manitoba Geological Survey, p. 129–144.

Summary

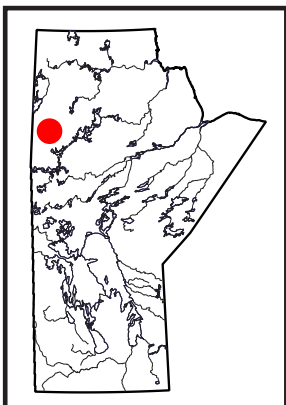
This report presents two new high-precision CA-ID-TIMS (chemical abrasion–isotope dilution–thermal ionization mass spectrometry) U-Pb zircon dates for two important granitoid intrusions from the Lynn Lake greenstone belt of the Paleoproterozoic Trans-Hudson orogen, northwestern Manitoba. Geochronological sampling was guided by detailed bedrock geological mapping and crosscutting relationships, which effectively constrained the temporal sequence of the dated granitoid intrusions relative to the surrounding country rocks. The leucogranite of the Little Brightsand Lake pluton, dated at 1848.3 ± 2.7 Ma, intrudes the Zed Lake group greywacke, which is comparable to the Sickle group sedimentary rocks. This provides not only a precise crystallization (and/or emplacement) age of the leucogranite but also establishes a minimum deposition age for the Zed Lake group greywacke. The quartz diorite of the Motriuk Lake pluton, dated at 1849.4 ± 1.3 Ma, cuts the Wasekwan group supracrustal package and displays an adakitic signature in its whole-rock geochemical composition, characteristic of post-arc slab failure granitoids. Geochemically, the Motriuk Lake quartz diorite is more primitive than the Little Brightsand Lake leucogranite. The two intrusions, while distinct in geochemical composition, are identical in age within their uncertainties and are therefore interpreted to be derived from distinct sources and emplaced in different geodynamic settings. The Motriuk Lake quartz diorite likely formed by post-arc magmatism triggered by slab break-off due to terrane collision during the Trans-Hudson orogeny, whereas the Little Brightsand Lake leucogranite originated from anatexis (or partial melting) of crustal materials. These new age data provide strong evidence for lithostratigraphic correlation, particularly for the period ca. 1857–1847 Ma in the region, and have significant implications for the understanding of diverse granitoid magmatism and its genetic link to orogenic gold mineralization in the Lynn Lake greenstone belt of the Paleoproterozoic Trans-Hudson orogen.

Introduction

In 2024, the Manitoba Geological Survey (MGS) continued its multiyear bedrock geological mapping program in the Paleoproterozoic Lynn Lake greenstone belt (LLGB), within the Trans-Hudson orogen of northwestern Manitoba. The objective of the fieldwork conducted in the summer of 2024 was to collect additional field data in support of the program's ultimate goal of updating 1:50 000 scale bedrock geology maps of the belt. This has involved examining key sites, continuing the ongoing compilation of existing data and incorporating newly acquired bedrock mapping information. Bulk-rock samples ($n = 29$) were collected from key exposures examined this past summer for further laboratory work. New field observations are highlighted below, in particular from the occurrences of diverse granitoid intrusions, which provide critical insights into the geodynamic evolution of the LLGB and genesis of the various types of economic mineralization at specific stages of the Trans-Hudson orogeny:

- A diorite stock cuts the Ralph Lake conglomerate, which is then cut by feldspar porphyry dikes.
- A leucogranite intrusion, part of the Little Brightsand Lake pluton, intrudes greywacke of the Zed Lake group.
- The Motriuk Lake pluton cuts the Wasekwan group volcanic and volcanoclastic to sedimentary sequence.
- A garnet-bearing S-type granodiorite phase in the Zed Lake pluton, cut by leucogranite dikes, has been identified.
- Muscovite-tourmaline pegmatite dikes cut volcano-sedimentary rocks of the Wasekwan group.

Based solely on the crosscutting relationships observed in the field, the Little Brightsand Lake granitoid intrusion in this report can be interpreted as postdating deposition of the Zed Lake group greywacke and the Motriuk Lake pluton as postdating Wasekwan group. The feldspar



porphyry dike and muscovite-tourmaline pegmatite dikes might be part of the Late intrusive suite that appear to be discrete in occurrence and do not show a certain connection with any large granitoid plutons (Yang, 2019, 2021a, 2023a; Yang and Beaumont-Smith, 2015, 2017). This study uses high-resolution, chemical-abrasion, isotope dilution–thermal ionization mass spectrometry (CA-ID-TIMS) U-Pb zircon geochronology to date the Motiuk Lake and Little Brightsand Lake plutons. The former cuts through the Wasekwan group (Yang, 2019), and the latter intrudes the Zed Lake group (Yang, 2021a). The new data provide a key piece of evidence for lithostratigraphic correlation in the region, geodynamic evolution, occurrences of diverse granitoid magmatism and their genetic linkages with potential economic mineralization, such as orogenic gold and rare metals or critical minerals. A revised tectonic model is proposed to demonstrate the geodynamic processes recorded in diverse granitoid intrusions and associated mineralization potential of the LLGB.

General geology

The LLGB, an important element of the Paleoproterozoic Trans-Hudson orogen (THO; Hoffman, 1988; Lewry and Collerson, 1990; Zwanzig, 2004; Ansdell, 2005; Corrigan et al., 2007, 2009; Zwanzig and Bailes, 2010; Corrigan, 2012), is endowed with several styles of economic mineralization, such as volcanogenic massive sulphide (VMS) zinc-copper (Zn-Cu), magmatic nickel-copper-cobalt (Ni-Cu-Co) and orogenic gold (Au; see Figure GS2024-16-1), as well as rare-earth elements and niobium hosted in the Eden Lake carbonatite complex (e.g., Mumin, 2002; Chakhmouradian et al., 2008). Mining in the Lynn Lake greenstone belt has historically contributed significantly to Manitoba's economy and continues to remain a primary focus for mineral exploration companies.

The LLGB is bounded to the north by the Southern Indian domain and flanked to the south by the Kiseynew domain (Gilbert et al., 1980; Gilbert, 1993; Zwanzig and Bailes, 2010; Martins et al., 2022). It is composed of two east- to northeast-trending, steeply dipping belts (Figure GS2024-16-1) consisting of various supracrustal rocks of the Wasekwan group that were intruded by granitoid plutons of the 1.891–1.870 Ga Pool Lake intrusive suite (Manitoba Energy and Mines, 1986; Baldwin et al., 1987; Turek et al., 2000; Beaumont-Smith and Böhm, 2002; Beaumont-Smith et al., 2006), which is believed to be pre-Sickle (e.g., Yang and Beaumont-Smith, 2015; Yang, 2023a). The Wasekwan group consists of a variety of volcanic rocks, including basalt, andesite, dacite, rhyolite and related volcanoclastic rocks, along with sedimentary rocks. Younger, molasse-type sedimentary rocks of the Sickle group (>1.836 Ga; see Lawley et al., 2020) unconformably overlie the Wasekwan group and the Pool Lake intrusive suite. Based on their crosscutting relationships with the Sickle group, the granitoid intrusions in the LLGB are divided into three intrusive suites: pre-Sickle, syn- to post-Sickle and late intrusions (Milligan, 1960; Yang and Beaumont-Smith, 2015, 2017;

Yang and Lawley, 2018, 2024a; Yang, 2019, 2021a, 2023a). The supracrustal rocks and the granitoid rocks of the LLGB experienced peak amphibolite-facies metamorphism ca. 1.83–1.81 Ga (Lawley et al., 2020, 2023). The lithostratigraphic column of the supracrustal sequence, including the Wasekwan and Sickle groups (as well as the Ralp Lake and Zed Lake groups, interpreted by some authors as comparable with the Sickle group; see Gilbert et al., 1980; Syme, 1985; Gilbert, 1993; Lawley et al., 2020, 2023), and their relationships with three intrusive suites of granitoid plutons and/or intrusions, are illustrated in Figure GS2024-16-2, which also highlights various styles of economic mineralization within the LLGB.

Significant differences in the geology and geochemistry of the northern and southern belts of the LLGB (Gilbert et al., 1980; Syme, 1985; Zwanzig et al., 1999; Beaumont-Smith, 2008; Glendenning et al., 2015) may reflect regional differences in tectonic settings obscured by structural transposition of multiple deformation events (D_1 – D_6 ; Zwanzig, 2000; Anderson and Beaumont-Smith, 2001; Beaumont-Smith and Böhm, 2002, 2003, 2004; Jones et al., 2006). The northern and southern belts contain disparate volcanic assemblages that were later structurally juxtaposed, likely representing a tectonic collage (Zwanzig et al., 1999) formed by northward subduction, followed by contraction and underthrusting of the Kiseynew domain beneath the LLGB during terminal collision (White et al., 2000). Note that this report uses the term 'Wasekwan group' to consist with publications released previously by the MGS (e.g., Gilbert et al., 1980; Gilbert, 1993; Syme, 1985; Baldwin et al., 1987; Beaumont-Smith and Böhm, 2002, 2003, 2004; Beaumont-Smith, 2008; Yang, 2023a, 2023b and references therein).

Field observations and historical drilling records indicate the presence of disseminated to massive sulphides (e.g., sphalerite, chalcopyrite, pyrrhotite) in the Wasekwan supracrustal rocks, including the Fox VMS Zn-Cu ore deposit (Gilbert et al., 1980; Fedikow and Gale, 1982; Baldwin, 1989; Ferreira, 1993; Yang and Beaumont-Smith, 2015, 2016; Yang, 2022, 2023b). These sulphide minerals, regardless from strata-bounded VMS deposits or country rocks, may have played an important role in the formation of magmatic Ni-Cu-Co ore deposits hosted in mafic-ultramafic intrusions (e.g., the Lynn Lake deposit; Figures GS2024-16-1 and -2) via providing external sulphur required for triggering sulphide saturation in tholeiitic (or calcic) gabbroic magmas (Yang, 2023b). Orogenic gold deposits in the LLGB, either intrusion-hosted or epigenetic, are controlled mostly by D_2 shear zones, although the intersections of D_3 or D_4 structures with D_2 faults could be favourable settings for Au further enrichment (i.e., chemical-structural traps; Beaumont-Smith and Böhm, 2004; Jones et al., 2006; Yang and Beaumont-Smith, 2015; Hastie et al., 2018; Lawley et al., 2020, 2023). Multiple phases of gold (Au) mineralization occurred up to 80 Myr after the peak of metamorphism (Figure GS2024-16-2), potentially as a result of the exhumation of the THO (see Lawley et al., 2023).

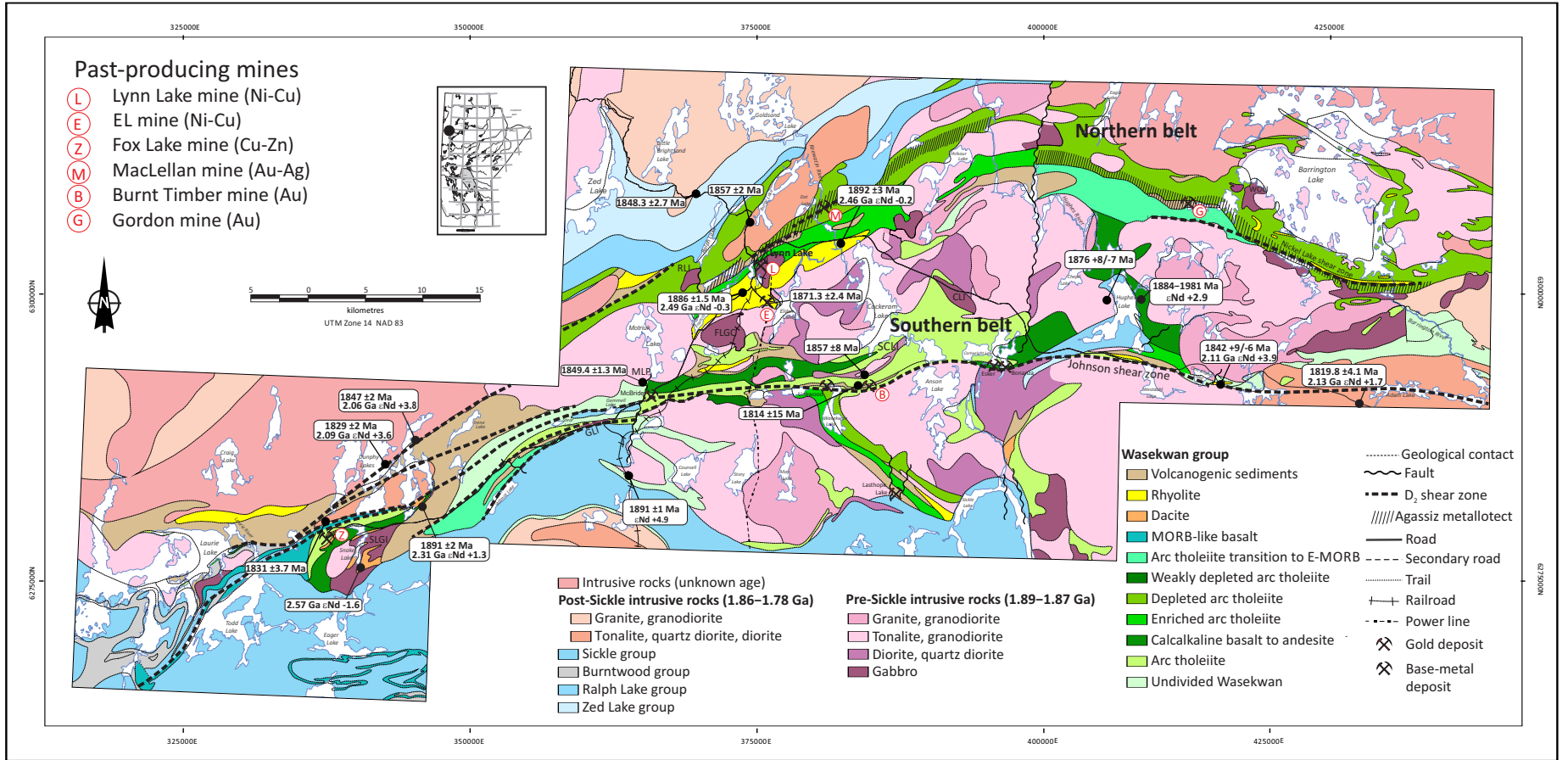


Figure GS2024-16-1: Regional geology with uranium-lead zircon ages and neodymium isotopic compositions of the Lynn Lake greenstone belt (modified and compiled from Gilbert et al., 1980; Manitoba Energy and Mines, 1986; Gilbert, 1993; Zwanzig et al., 1999; Turek et al., 2000; Beaumont-Smith and Böhm, 2002, 2003, 2004; Beaumont-Smith et al., 2006; Jones et al., 2006; Beaumont-Smith, 2008; Yang and Beaumont-Smith, 2015, 2016, 2017; Lawley et al., 2020, 2023; Yang, 2022, 2023b). Abbreviations: CLI, Cartwright Lake intrusion; FLGC, Fraser Lake gabbro complex; GLI, Gemmell Lake intrusion; MLP, Motriuk Lake plug; MORB, mid-ocean-ridge basalt; RLI, Ralph Lake intrusion; SCL, Southern Cockeram Lake intrusion; SLGI, Snake Lake gabbro intrusion; WOLI, White Owl Lake intrusion.

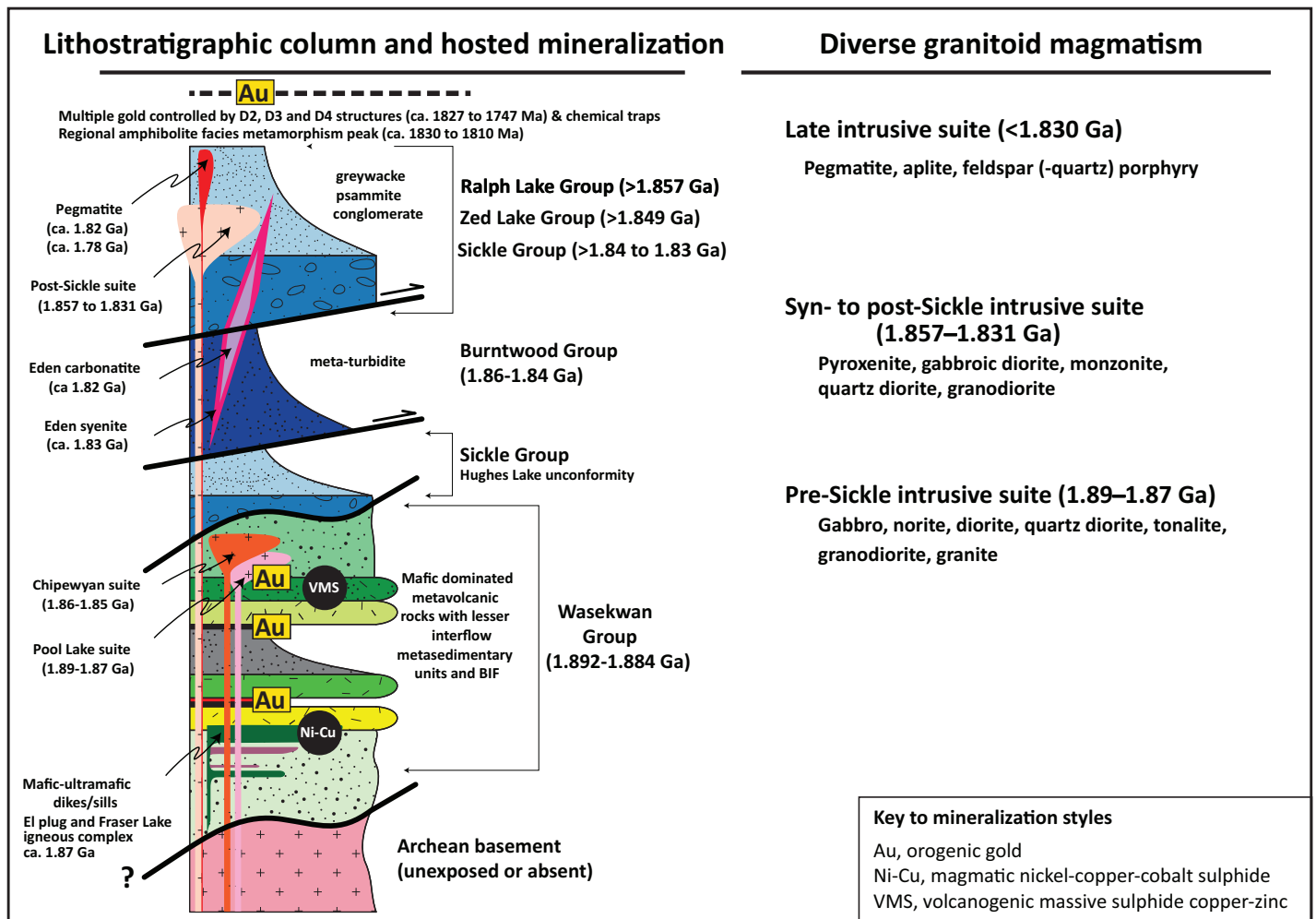


Figure GS2024-16-2: Schematic lithostratigraphic column of the Lynn Lake greenstone belt, intruded by three suites of various styles of granitoid intrusions and related (or) hosted mineralization based on the field relationships, detailed bedrock geological mapping, new and published U-Pb zircon geochronological data (modified after Lawley et al., 2020, 2023; Yang, 2019, 2023a; this study). Abbreviation: BIF, banded iron formation.

Sample descriptions

Two granitoid samples were dated to establish precise age constraints on the timing of their crystallization and/or emplacement. One sample (111-19-350A01) is a quartz diorite collected from the Motriuk Lake pluton that cuts the supracrustal sequence of the Wasekwan group (Yang, 2019). This quartz diorite is massive, medium-grained, moderately to weakly foliated and equigranular, displaying relatively high magnetic susceptibility (MS) values of up to 7.6×10^{-3} SI indistinguishable from normally oxidized magnetite-series and normal I-type granites elsewhere (Chappell and White, 1974, 1992, 2001; Ishihara, 1977, 1981, 2004; Yang, 2023a). It consists of 5-10% quartz (~3-4 mm), 60-70% plagioclase laths (3-5 mm), and 15-20% amphibole with diffuse crystal edges (2-5 mm; Figure GS2024-16-3a), and accessory minerals including Fe-Ti oxides, zircon, titanite, and apatite.

The other sample dated in this study is a leucogranite (111-21-154A01) that was collected from the Little Brightsand Lake pluton intruding the Zed Lake group greywacke (Yang, 2021a). This leucogranite is medium- to coarse-grained, massive, equigranular and locally porphyritic, having low MS value of

0.054×10^{-3} SI, much similar to reduced ilmenite series and S-type granites (Chappell and White, 1974, 1992, 2001; Ishihara, 1977, 1981, 2004; Yang, 2023a). It consists of 25-35% anhedral quartz (2-4 mm), 55-60% subhedral to euhedral feldspar (2-4 mm), 4-5% biotite and about ~1% muscovite (Figure GS2024-16-3b). The contact between the greywacke and the leucogranite is sharp and wavy to irregular, and concentrates biotite aggregates on the greywacke side, typical of contact metamorphism caused by the leucogranite intrusion (Yang, 2021a). The leucogranite becomes finer in grain size as it approaches the contact with the Zed Lake greywacke. It occurs as dikes and/or veins that seem to have been emplaced along S_2 foliations, which are folded into 'Z' shapes and boudinaged together with quartz veins containing pyrite (Figure GS2024-16-3c, d). This suggests that the leucogranite is syn-kinematic and likely influenced by trans-compression during terrane collision.

Geochemical attributes

Granitoid samples from the Motriuk Lake and Little Brightsand Lake plutons exhibit distinctly different geochemical char-

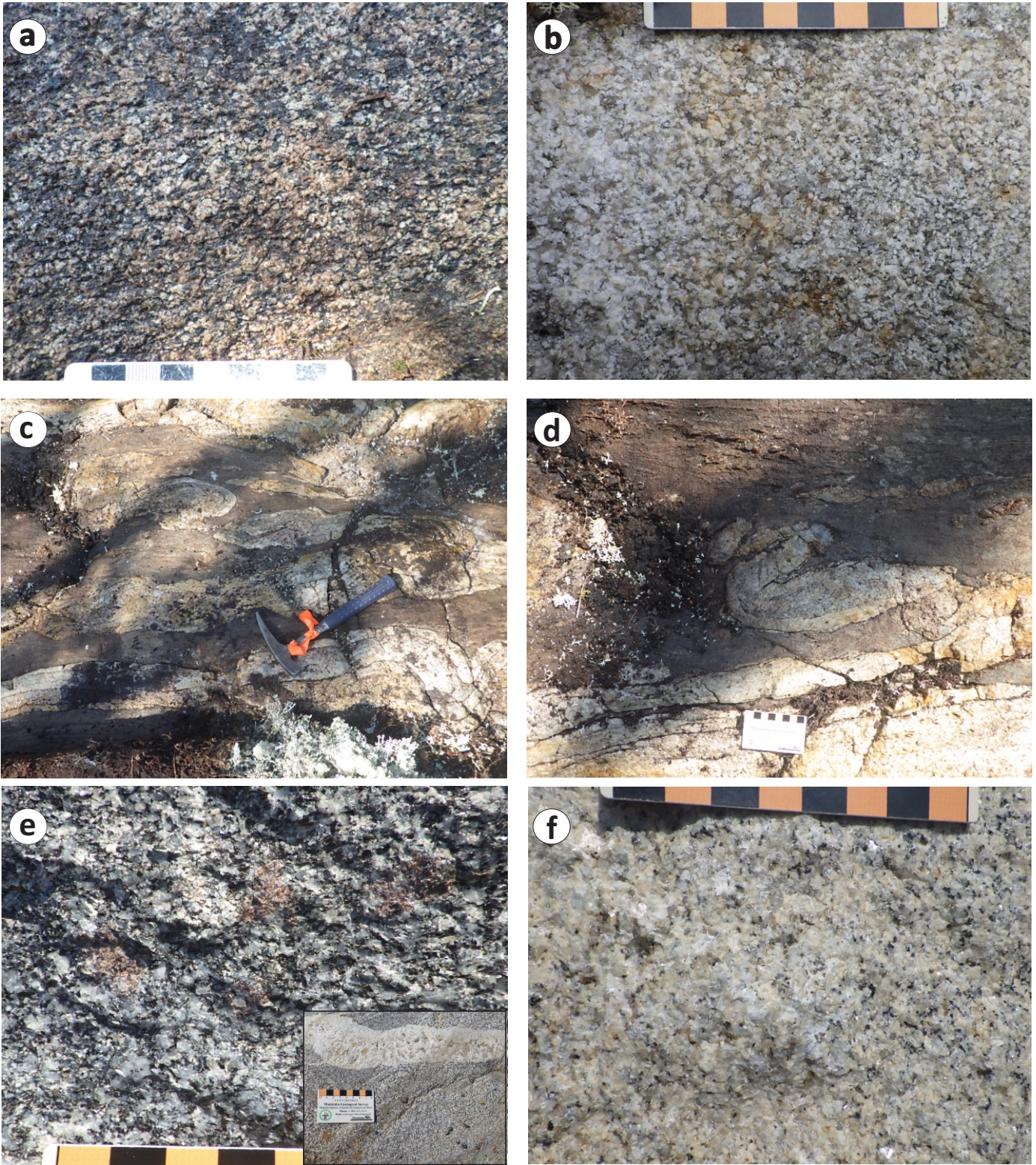


Figure GS2024-16-3: Field photos of granitoid rocks showing textural features and field relationships, and the rocks sampled for precise U-Pb zircon age determination: **a)** medium-grained quartz diorite from the Motriuk Lake pluton (UTM Zone 14, 365250E, 6292311N, NAD 83); **b)** massive, equigranular, medium- to coarse-grained leucogranite from the Little Brightsand Lake pluton (UTM 369166E; 6308570N) with MS value of 0.054×10^{-3} SI; **c)** the leucogranite dikes and/or veins cut the Zed Lake greywacke that has higher MS value of 0.348×10^{-3} (UTM 365250E, 6292311N); **d)** the leucogranite dikes and veins are folded (e.g., as 'Z'-shaped fold) and boudinaged. UTM co-ordinates are the same as the exposure of (c); hammer handle points north; **e)** medium-grained garnet-bearing granodiorite (MS value of 0.44×10^{-3}) from the Zed Lake pluton (UTM 363768E, 6314725N), which is cut by a medium- to coarse-grained leucogranite dike as shown by inset photo in the lower right corner; note that reddish garnet presents mainly as garnet + biotite + feldspar aggregates, although discrete garnet crystals are also evident; and **f)** medium- to coarse-grained leucogranite (MS value of 0.041×10^{-3}) UTM locality is the same as (e).

acteristics (Figure GS2024-16-4; the data from Yang, 2020, 2021b, 2024). The Motriuk Lake samples have relatively lower and varied SiO₂ contents and range from diorite to granodiorite and granite, according to the total alkalis versus silica (TAS) classification diagram (Figure GS2024-16-4a) proposed by Middlemost (1994). These samples display a mainly calcalkaline affinity, with one exception that is calcic or tholeiitic based on the Rittmann serial index ($\sigma < 1.2$; Yang, 2007). They are mainly metaluminous, as indicated by the Shand index diagram (Figure GS2024-16-4b) and less evolved in geochemical composition, as suggested by lower τ^1 values (22.1–53.0). Additionally, the Motriuk Lake samples show high Sr/Y (>40) and La/Yb (>20) ratios (Figure GS2024-16-4c), which are characteristic of adakite-like granitoids and/or sanukitoids (Shirey and Hanson, 1984; Martin et al., 2005, 2009; Richards and Kerrich, 2007; Yousefi and Lentz, 2024) or slab-failure granitoids (Hildebrand et al., 2018; Yang and Lawley, 2018, 2024a, 2024b; Whalen and Hildebrand, 2019).

The granitoid samples from the Little Brightsand Lake pluton are exclusively situated in the granite field on the TAS diagram and are predominantly calcic in magmatic affinity (Figure GS2024-16-4a). They are classified as peraluminous granites based on the Shand index (Figure GS2024-16-4b). All four samples display low La/Yb ratios (<20) and an exceptionally wide range of Sr/Y ratios, from 6 to 1436, with some values plotting beyond the scale of Figure GS2024-16-4c. These geochemical signatures suggest the significant presence of feldspar cumulates in the rocks. This is supported further by their calcic (or tholeiitic) magmatic affinity combined with highly evolved geochemical characteristics, as indicated by their high SiO₂ concentrations (73.4 wt. % to 74.5 wt. %) and high τ values (54.4 to 241.4).

U-Pb zircon dating

Precise U-Pb zircon ages from episodic granitoid magmatism is crucial in understanding the geodynamic settings recorded by granitoids in mountain belts, such as the Paleozoic Appalachian Mountains (e.g., Frisch et al., 2011), the Paleoproterozoic Trans-Australian Orogen (Gibson et al., 2024), and the Paleoproterozoic Trans-Hudson orogen (Beaumont-Smith and Böhm, 2002; Beaumont-Smith et al., 2006; Yang and Lawley, 2018). A variety of genetic types of granitoids have been identified thus far in the LLGB of the Manitoban THO, such as volcanic arc I-type, intra-arc extensional A-type, and adakite-like (or adakitic) granitoids intrusions as well as collisional S-type granites (Yang, 2019, 2021a, 2023a; Yang and Lawley, 2018, 2024a, 2024b; see Figure GS2024-16-3a to -3f). As mentioned above, these diverse granitoids can be grouped into pre-Sickle, syn- to post-Sickle and late intrusive suites (Figure GS2024-16-2).

¹ $\tau = (\text{Al}_2\text{O}_3 - \text{Na}_2\text{O})/\text{TiO}_2$, unit in wt. %. τ was proposed by (Grasso, 1968), that is termed Gottini index and can be used readily for describing degree of magmatic differentiation (Yang, 2007). A higher τ value signifies a greater level of differentiation.

Methods

U-Pb zircon geochronological analysis was performed at the Jack Satterly Geochronology Laboratory, the University of Toronto, Ontario (Canada), using chemical abrasion- isotope dilution-thermal ionization mass spectrometry (CA-ID-TIMS) dating techniques with high precision. Whole-rock samples are initially crushed and ground into powder, followed by heavy mineral separation using a Wilfley table and further purification through density and magnetic separations. Zircon, the target mineral, is selected manually under a binocular microscope to ensure the freshest and least altered grains are chosen (see Hamilton, 2022).

The selected zircon grains undergo chemical abrasion to remove radiation-damaged areas, following a modified procedure after Mattinson (2005). This involves annealing the grains at 900°C for two days and etching them in hydrofluoric acid. The chemically abraded grains are then dissolved, and uranium (U) and lead (Pb) are isolated using anion exchange columns as described by Krogh (1973). The isotopic compositions of Pb and UO₂ are analyzed using a VG354 mass spectrometer with a Daly collector, following the methodology outlined by Gerstenberger and Haase (1997).

The mass spectrometer data is processed using the UtilAge program developed by D. Davis, with corrections for initial ²³⁰Th disequilibrium in zircon applied to the ²⁰⁶Pb/²³⁸U ages, assuming a Th/U ratio in the magma of 4.2 (Hamilton, 2022). Common Pb is assigned to procedural blank, and initial Pb above 1 picogram is corrected using the Pb evolution model by Stacey and Kramers (1975). The analytical results are tabulated in Table GS2024-16-1. The Concordia curve is plotted using the Isoplot 3.71 Add-In for MS Excel® program (Ludwig, 2009), incorporating uncertainties in uranium decay constants (Jaffey et al., 1971). Ages are reported with a 95% confidence level, and complex cases are discussed in detail (below).

Results

Quartz diorite (sample 111-19-350A01) from the Motriuk Lake pluton

Abundant zircon crystals were yielded from least magnetic fraction of the heavy mineral concentrate from the quartz diorite sample 111-19-350A01. These zircon crystals are nearly pure, fine-grained, and dominated by colourless to very pale yellow, clear to slightly clouded, short to elongate (up to 5:1) prismatic morphologies, commonly with cracks. These features are common for magmatic zircons (Corfu et al., 2003). Four pristine zircon crystals (see inset photos a and b of Figure GS2024-16-5) were selected for U-Pb chemical and isotope analysis. Minor molybdenite is present in the mineral separates, as is well-formed dark and pale titanite in the more magnetic fractions.

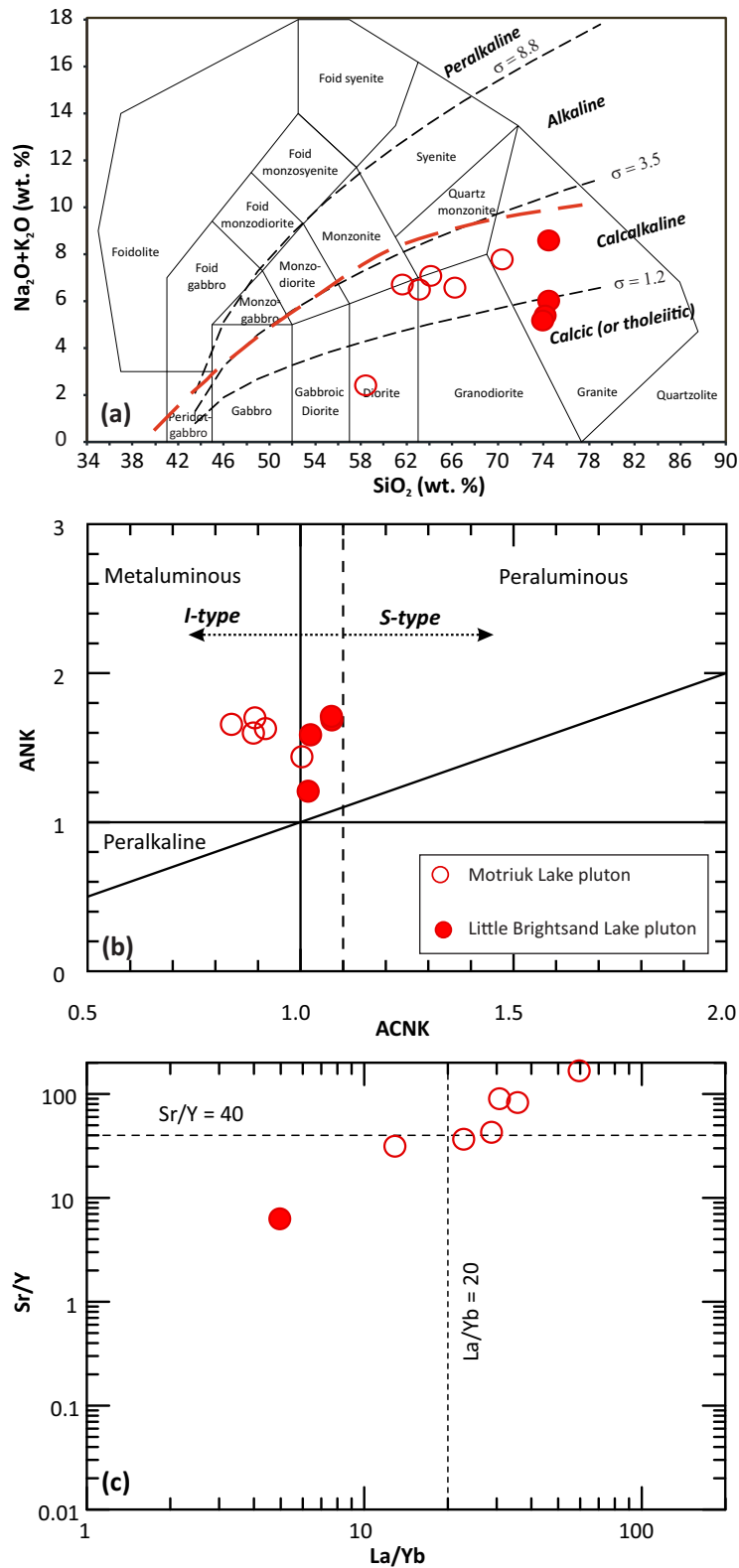


Figure GS2024-16-4: Geochemical characteristics of granitoid rocks: **a)** total alkalis versus SiO_2 diagram (TAS; after Middlemost, 1994); dashed lines labeled σ values indicate the boundaries between calcic ($\sigma \leq 1.2$), calc-alkaline ($1.2 < \sigma < 3.5$), alkaline ($3.5 < \sigma < 8.8$), and peralkaline series ($8.8 \leq \sigma$) (after Yang, 2007); σ denotes the Rittmann Serial index, and $\sigma = (\text{Na}_2\text{O} + \text{K}_2\text{O})^2 / (\text{SiO}_2 - 43)$, unit in wt. % (Rittmann, 1962, 1973); red dashed line is boundary of subalkaline and alkaline volcanic rocks (Irvine and Barager, 1971). **b)** Shand index plot based on ANK versus ACNK (after Maniar and Piccoli, 1989); $\text{ACNK} = \text{molar Al}_2\text{O}_3 / (\text{CaO} + \text{Na}_2\text{O} + \text{K}_2\text{O})$, $\text{ANK} = \text{molar Al}_2\text{O}_3 / (\text{Na}_2\text{O} + \text{K}_2\text{O})$; vertical dashed line is $\text{ACNK} = 1.1$ discriminating S- from I-type granites (after Chappell and White, 1974, 2001). **c)** Sr/Y versus La/Yb ratios for discrimination of adakites from arc rocks (after Richards and Kerrich, 2007); note that three samples from the Little Brightsand Lake pluton plot out of Y-axis as they have Sr/Y ratios of 647 to 1436 but low La/Yb (< 20), suggestive of the occurrence of significant amounts of feldspar cumulates (data sources: Yang, 2020, 2021b, 2024).

Table GS2024-16-1: Chemical abrasion–isotope dilution–thermal ionization mass spectrometry (CA-ID-TIMS) U-Pb isotopic data for zircons in the granitoids samples from the Lynn Lake greenstone belt.

Sample/ Fraction	Description	U (ppm)	Th/U	Pb ¹ (pg)	Pb _c (pg)	²⁰⁶ Pb/ ²⁰⁴ Pb	²⁰⁷ Pb/ ²³⁵ U	±2σ	²⁰⁶ Pb/ ²³⁸ U	±2σ	Corr. Coeff. (rho)	²⁰⁷ Pb/ ²⁰⁶ Pb	±2σ	²⁰⁷ Pb/ ²³⁵ U	±2σ	²⁰⁶ Pb/ ²³⁸ U	±2σ	²⁰⁷ Pb/ ²⁰⁶ Pb	±2σ	Disc. (%)
<i>Motriuk Lake quartz diorite (sample 111-19-350A01; UTM Zone 14, 365250E, 6292311N, NAD 83)</i>																				
Z1	1 clr, cls, flat, shrt pr; incl	310	0.456	108.7	0.50	13046	5.17896	0.01922	0.332161	0.000866	0.7439	0.113082	0.000281	1849.2	3.2	1848.8	4.2	1849.5	4.5	0.0
Z2	1 clr, cls, el (2.5:1) pr; incl	271	0.430	47.86	0.35	8271	5.17568	0.01297	0.331983	0.000679	0.9111	0.113071	0.000120	1848.6	2.1	1848.0	3.3	1849.3	1.9	0.1
Z3	1 clr, cls, brkn el pr, crkd; dk incl	171	0.480	62.36	11.27	338	5.19269	0.08079	0.332697	0.001238	0.6804	0.113199	0.001508	1851.4	13.3	1851.4	6.0	1851.4	24.2	-0.0
Z4	1 clr, cls, crkd flat pr	340	0.439	138.0	1.28	6521	5.17664	0.01334	0.332008	0.000676	0.9102	0.113083	0.000126	1848.8	2.2	1848.1	3.3	1849.5	2.0	0.1
<i>Little Brightsand Lake leucogranite (sample 111-21-154A01; UTM Zone 14369166E, 6308570N, NAD 83)</i>																				
Z1	1 c-e, cls-grey brkn needle, tip	40	0.046	13.1	1.00	888	5.22109	0.03818	0.335048	0.001152	0.6689	0.113019	0.000636	1856.1	6.2	1862.8	5.6	1848.5	10.2	-0.9
Z2	2 cls, cls flat/el, crkd pr	52	0.040	16.8	0.92	1224	5.18501	0.06047	0.332469	0.003484	0.9242	0.113109	0.000505	1850.2	9.9	1850.3	16.9	1850.0	8.1	-0.0
Z3	1 c-e, cls-grey, brkn, el, oz pr	124	0.087	40.3	0.78	3393	5.17291	0.01705	0.332030	0.000844	0.8565	0.112994	0.000195	1848.2	2.8	1848.2	4.1	1848.1	3.1	-0.0
Z4	1 clr, cls, crkd, flat, brkn, el pr tip	44	0.051	14.1	1.40	682	5.18691	0.04715	0.333003	0.001147	0.6481	0.112969	0.000830	1850.5	7.7	1852.9	5.5	1847.7	13.3	-0.3

Notes:

All analyzed zircon fractions represent best optical quality (crack, inclusion, and core free), freshest (least altered) available grains. All zircons were chemically abraded.

Abbreviations: anh, anhedral; brkn, broken; c-e, cloudy-etched; cld, clouded/turbid; clr, clear; cls, colourless; crkd, cracked; dk, dark; dt, doubly-terminated; el, elongate; eq, equant; ext, exterior/outermost; fctd, faceted; frag, fragment(s); gl, glassy; incl, mineral or melt inclusion(s); irr, irregular; lrg/med/sm, larger/medium/smaller; oz, oscillatory-zoned; pbr, pale brown; pr, prism/prismatic; shrp, sharp; shrt, short; skel, skeletal; sl rnd, slightly rounded; Z, zircon.

Pb^T is total amount (in picograms) of Pb.

Pb_c is total measured common Pb (in picograms) assuming the isotopic composition of laboratory blank: ²⁰⁶Pb/²⁰⁴Pb - 18.49 ±0.4%; ²⁰⁷Pb/²⁰⁴Pb - 15.59 ±0.4%; ²⁰⁸Pb/²⁰⁴Pb - 39.36 ±0.4%.

Pb/U atomic ratios are corrected for spike, fractionation, blank, and, where necessary, initial common Pb; ²⁰⁶Pb/²⁰⁴Pb is corrected for spike and fractionation.

Th/U is model value calculated from radiogenic ²⁰⁸Pb/²⁰⁶Pb ratio and ²⁰⁷Pb/²⁰⁶Pb age, assuming concordance.

Disc. (%) - per cent discordance for the given ²⁰⁷Pb/²⁰⁶Pb age.

Uranium decay constants are from Jaffey et al. (1971).

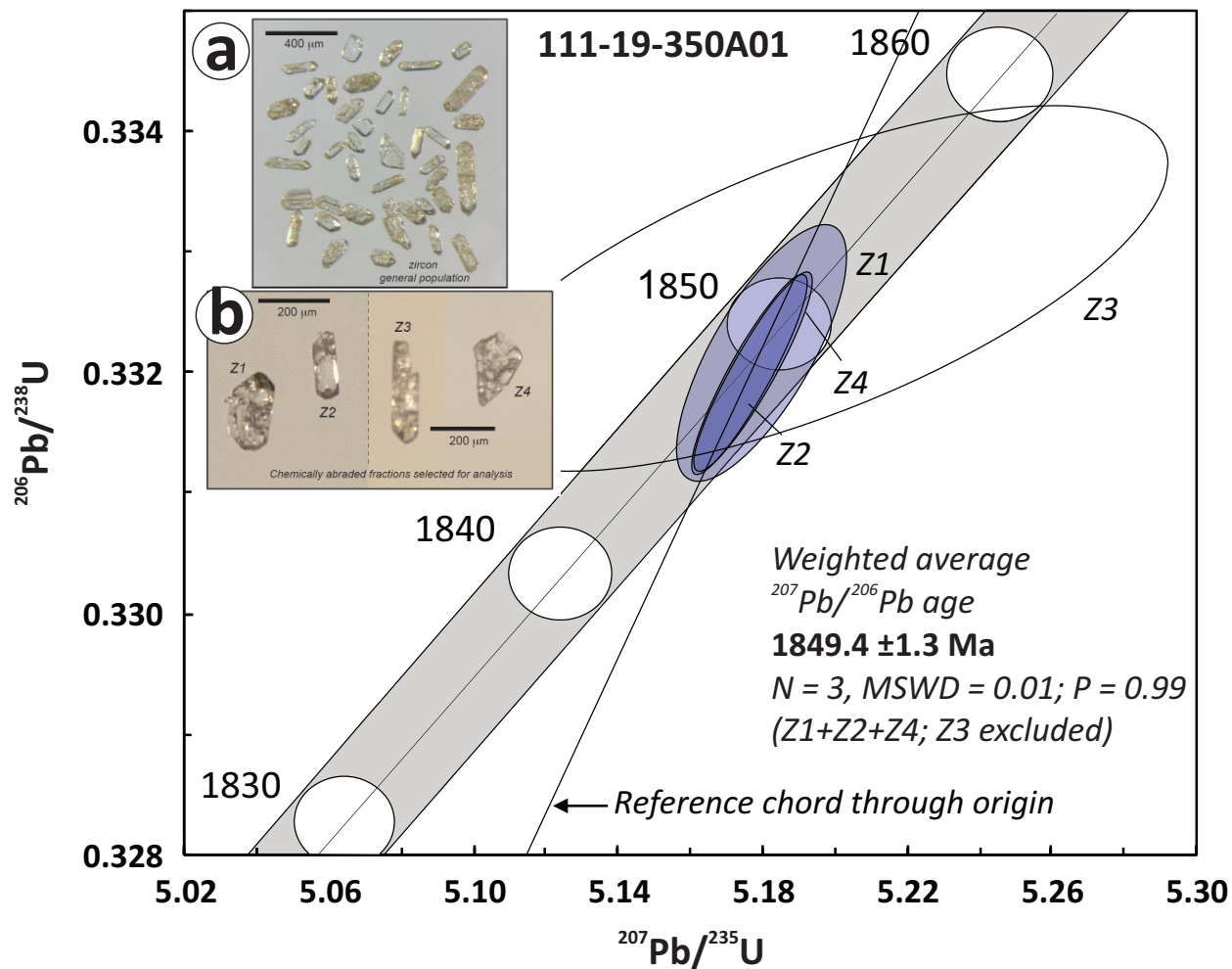


Figure GS2024-16-5: Concordia diagram of CA-ID-TIMS U-Pb zircon age data for quartz diorite sample from the Motriuk Lake pluton in the Lynn Lake greenstone belt. Inset photos show population of zircons recovered from the sample (a) and chemical abraded and analysed zircon grains (b). Abbreviations: MSWD, mean squares of weighted deviates; N, number of analyses; P, probability.

U-Pb isotopic results are presented for the analyzed four single grain zircon fractions in Table GS2024-16-1 and plot on Figure GS2024-16-5. The data points for all fractions are concordant and overlapping, although the results for Z3 are imprecise due to elevated common Pb, likely resulting from the presence of micro-inclusions in it. Nevertheless, calculated $^{207}\text{Pb}/^{206}\text{Pb}$ ages for all four analyses range narrowly between 1849.3 and 1851.4 Ma, and between 1849.3 and 1849.5 Ma when excluding Z3. A weighted average age calculated for Z1, Z2 and Z4 gives 1849.4 ± 1.3 Ma (MSWD = 0.01; P = 99%). This age is considered a robust age for the timing of crystallization and/or emplacement of the quartz diorite. This age certainly fits within the intermediate age interval of felsic plutonism in the Lynn Lake greenstone belt (e.g., 1857 to 1847 Ma; Figure GS2024-16-2). It is also similar to the older age for the northeast Dunphy Lakes hornblende tonalite, at 1847 ± 2 Ma reported by Beaumont-Smith and Böhm (2003). Note that Beaumont-Smith and Böhm (2003) also reported a slightly younger age of ca. 1843 Ma for a rhyodacite sample collected from One Island Lake to east of the LLGB (see Figure

GS2024-16-1), that seems to be product of a distinct episode of magmatism from the Motriuk Lake adakitic plutonism.

Leucogranite (sample 111-21-154A01) from the Little Brightsand Lake pluton

This leucogranite sample gave a good recovery of zircon grains, with the population dominated by elongate, colourless to pale- and medium-yellow, clear to clouded, frequently cracked crystals (see inset photos a and b in Figure GS2024-16-6).

A total of four fractions were analyzed from this sample, each comprising 1 or 2 grains; the results are all overlapping and mostly concordant (Table GS2024-16-1; Figure GS2024-16-6). Most of the zircon crystals appear to be relatively low in U (much like the whole rock) and nonradiogenic for Pb, so that the individual analyses have slightly expanded error ellipses, but the $^{207}\text{Pb}/^{206}\text{Pb}$ ages are all very consistent between 1847.7 and 1850.0 Ma. The analyzed zircons are also very depleted in Th, giving uniformly low Th/U ratios between 0.04 and 0.09 (Table GS2024-16-1). Collectively, all four analyses yield a weighted

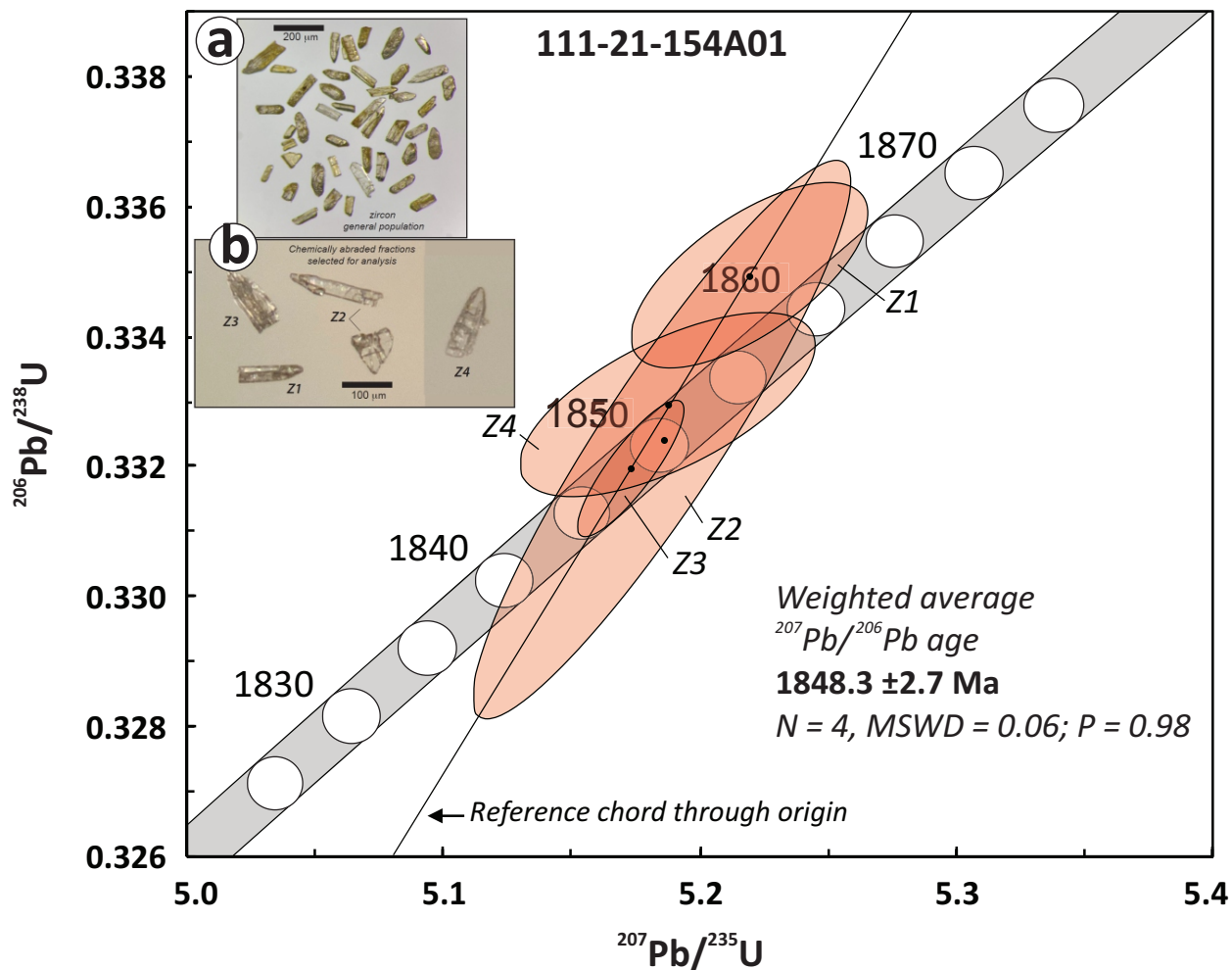


Figure GS2024-16-6: Concordia diagram of CA-ID-TIMS U-Pb zircon age data for the granite sample collected from the Little Brightsand Lake pluton in Ralph Lake mapping area (Yang, 2021a), Lynn Lake greenstone belt. Inset photos show population of zircons recovered from the sample (a) and chemical abraded zircon grains (b). Abbreviations: MSWD, mean squares of weighted deviates; N, number of analyses; P, probability.

average $^{207}\text{Pb}/^{206}\text{Pb}$ age of 1848.3 ± 2.7 Ma (MSWD = 0.06; P = 98%). This age is statistically identical within error to the new age presented above for sample 111-19-350A01 (1849.4 ± 1.3 Ma) but is younger than the 1857 ± 2 Ma Burge Lake pluton (Beaumont-Smith et al., 2006) that cuts the Ralph Lake group conglomerate (Yang and Beaumont-Smith, 2015).

Interpretation and geological significance

The U-Pb zircon age of 1849.4 ± 1.3 Ma for the quartz diorite of the Motriuk Lake pluton is interpreted as the timing of its crystallization and/or emplacement, which intrudes the Wasekwan group supracrustal package. This quartz diorite exhibits an adakitic geochemical signature (Yang and Lawley, 2024b; this study), geochemically consistent with post-arc slab failure granitoids described by Whalen and Hildebrand (2019). It is less evolved than the leucogranite in the Little Brightsand pluton. The adakitic intrusions are interpreted as products of post-arc magmatism, based on the tectonic model proposed by Hildebrand et al. (2018) and supported by observations from this study. Notably,

Zwanzig (2024) uses slab failure granitoid intrusions as indicators of terrane accretion to collisions during the tectonic evolution of the THO. Regardless of how the rocks are termed, the discovery of adakitic granitoids in the LLGB holds significant implications for gold mineralization, as several auriferous quartz-sulphide vein systems hosted in quartz diorite (e.g., McBride, Finlay McKinlay; see Yang, 2019) are located near the Motriuk Lake pluton. Similar spatial associations between adakitic intrusions and gold deposits have been observed at the Gordon Au mine adjacent to the Farley Lake stock, and at the McLellan Au-Ag mine alongside the Burge Lake pluton (see Yang and Lawley, 2018, 2024a, 2024b).

The U-Pb zircon age of 1848.3 ± 2.7 Ma for the leucogranite of the Little Brightsand Lake pluton is interpreted as the timing of its crystallization (and/or emplacement) within the Zed Lake group greywacke. This age also establishes a minimum deposition age for the Zed Lake greywacke. It has been postulated that the Sickle group sedimentary rocks are comparable in stratigraphic position and/or in age to the Zed Lake group greywacke (Gilbert et al., 1980; Syme, 1985; Gilbert, 1993; Yang and Beau-

mont-Smith, 2015; Lawley et al., 2020, 2023). If this is the case, the precise U-Pb zircon age reported here could indicate that the Sickie group deposition interval is not as well constrained as the narrow time interval of ca. 1.84-1.83 Ma interpreted by Lawley et al. (2020, 2023; Figure GS2024-16-2).

The reason for the relatively low Th/U ratios in zircon (Table GS2024-16-1) from the Little Brightsand Lake granite is unclear. If this granite crystallized from a peraluminous melt that was co-crystallizing high-Th monazite, low Th/U ratios in zircon precipitating from the melt would be expected. However, the geochemistry of this granite argues against such a scenario, consistent with the fact that there is no monazite observed. Rather, it appears to indicate the presence of cumulative feldspars from highly evolved granites. Zircon with Th/U ratios of <0.1 is common mostly in low-temperature and low-pressure metamorphic rocks and/or due to alteration itself (see Rubatto, 2017). If the granite melt formed by anatexis (or partial melting) of metamorphic rocks in the crust, it may have resulted in crystallization of zircon with such low Th/U ratios. Alternatively, highly evolved granite involved in Th-rich phases, such as monazite, allanite, could also lead to formation of zircon with low Th/U ratio. However, these accessory minerals are not evident in the leucogranite.

Tectonic model

A revised model of the tectonic evolution of the LLGB and adjacent domains/terrane is illustrated in Figure GS2024-16-7. This model considers the episodic and diverse granitoid magmatism of various genetic types (Figure GS2024-16-2), supported by precise U-Pb zircon age constraints. The tectonic evolution recorded in the LLGB is characterized by volcanic arc I-type granitoids, A-type granitoids associated with intraoceanic extension due to slab roll-back, and adakitic granitoids (e.g., the Farley Lake quartz diorite stock, the Burge Lake pluton, the Motriuk

Lake pluton, the Dunphy Lakes batholith, and the Fox mine intrusion; see Yang and Lawley, 2024a, 2024b, and this study) formed by partial melting of prior metasomatized depleted mantle triggered by slab break-off due to terrane collision. Terrane collision is indicated by the presence of S-type granitoids as described this past summer (Figure GS2024-16-3e; e.g., Yang et al., 2019; Yang, 2023a) but this finding needs to be backed up by precise U-Pb zircon geochronology, whole-rock geochemistry and tracer Sm-Nd isotopes. More importantly, this shift in geodynamic settings, in response to crust-mantle interactions through trans-crustal structures (e.g., the Nickel Lale shear zone, Johnson shear zone; Figure GS2024-16-1), particularly during specific stages, may have led to economic mineralization. Examples include arc I-type intrusions associated with porphyry Cu-Au-Mo (cf. Richards and Kerrich, 2007; Sun et al., 2010; Yousefi and Lentz, 2024), A-type granites associated with U, Nb, and rare-earth elements (Whalen et al., 1987; Eby, 1990, 1992; Bonin, 2007), adakitic intrusions associated with Au (Cu) (Lin and Beakhouse, 2013; Whalen and Hildebrand, 2019), and collisional S-type granites associated with critical metals, such as Li, Ta, Cs, and Sn (see Yang et al., 2019; Yang and Lawley, 2024a and references therein). Association of S-types granites with pegmatite-hosted Li, Ta, Cs and Sn mineralization is currently not known in the LLGB. Further work is needed to establish this connection.

The ca. 1.857 (i.e., Burge Lake pluton; Beaumont-Smith, 2006) to 1.831 Ga (i.e., Fox mine intrusion; Turek et al., 2000), episodic adakite-like granitoid intrusions in the LLGB were formed as results of post-arc magmatism (Yang and Lawley, 2024b; this study), and likely indicates opposing subduction polarity (Figure GS2024-16-7); an older southward subduction; and a younger northward subduction. The current model proposal is consistent with the views of Corrigan et al. (2009) and Corrigan (2012), although their studies did not report the occurrences of adakitic granitoid intrusions. The arc magmatic activity

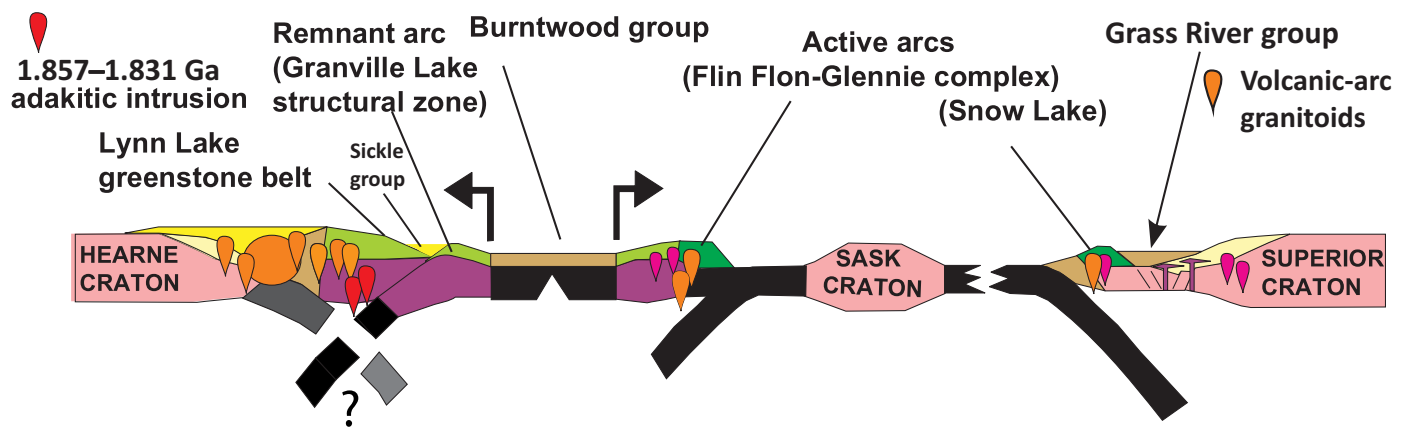


Figure GS2024-16-7: A revised tectonic model of the Lynn Lake greenstone belt (modified from Corrigan et al., 2007, 2009; Zwanzig and Bailes, 2010 and with results from this study). Slab break-off (dark grey) occurs as a result of terrane collision between a continental block and an oceanic arc, following an earlier southward subduction. A second slab break-off event (black) is caused by terrane collision, possibly between a continental arc and an oceanic arc, following a later northward subduction.

produced the 1.891 to 1.870 Ga Pool Lake intrusive suite, the pre-Sickle intrusions (Figure GS2024-16-2; Baldwin et al., 1987; Turek et al., 2000; Beaumont-Smith and Böhm, 2002; Beaumont-Smith et al., 2006; Manitoba Agriculture and Resource Development, 2021; Yang, 2023a). Geochemical and Nd isotopic analyses suggest that these adakitic granitoids may have originated from the partial melting of previously metasomatized mantle by subduction-related melts and/or fluids. This process was triggered by the upwelling of hot asthenospheric mantle due to slab roll-back and break-off events that were likely the consequences of terrane amalgamation or collision (Yang and Lawley, 2024a, 2024b).

The shifts of tectonic settings likely reflect a geodynamic response to deep mantle processes, creating an extensional setting within the uplifting orogen and leading to the formation of syn-orogenic basins filled with molasse-type sediments, such as the Sickle group polymictic conglomerate and arkosic sandstone. Concurrently, the exhumation of the Trans-Hudson orogen triggered gold mineralization (Lawley et al., 2023). Although the adakitic intrusions were emplaced before the onset of gold mineralization, auriferous fluids driven by magmatism would have flowed along the same deep faults where the intrusions occurred. As a result, these adakitic intrusions may serve as valuable indicators for targeting potential orogenic gold mineralization in the Lynn Lake greenstone belt and beyond in the Trans-Hudson orogen.

The syn-orogenic sedimentary basin filled by the Sickle group sediments represents a surface expression and response to deep geodynamic processes within the lithosphere of the orogenic belts (e.g., Lawley et al., 2020, 2023; Yang and Lawley, 2024a, 2024b; Gibson et al., 2024). Such model of a basin formation is attributed to extension, driven by slab roll-back and/or slab break-off, which induced magmatism represented by adakite-like granitoid intrusions (as well as A-type granites) simultaneously and may have initiated the flow of ore fluids into favourable structural-chemical traps, leading to gold mineralization in the Lynn Lake greenstone belt.

The field observations presented in this report along side the geochronology results suggest that the Sickle group was deposited during a longer time interval and may have been not only limited to the time interval of greater than ca. 1.84–1.83 Ga (Lawley et al., 2020, 2023). Alternatively, although the Sickle group in the LLGB is thought equivalent in depositional ages to the Ralph Lake and Zed Lake groups sedimentary rocks, the latter two were thought to deposit as part of the Southern Indian domain (SID; Manitoba Energy and Mines, 1986) and may not be correlated directly to the Sickle group. The boundary between the LLGB and the SID is represented by the Ralph Lake shear zone, where the Ralph Lake conglomerate and grey-

wacke are thrust over the Wasekwan group of the LLGB (e.g., Yang, 2021b).

Economic considerations

Syn- to post-Sickle group adakitic granitoid intrusions exhibit distinct geochemical characteristics compared to the highly differentiated leucogranites dated in this study, despite their synchronous occurrence within the LLGB. This difference underscores the diversity of post-arc granitoid magmatism linked to the geodynamic evolution of the Trans-Hudson orogen. The 1849.4 ±1.3 Ma quartz diorite of the Motriuk Lake pluton, an adakitic intrusion, likely formed through partial melting of a metasomatized mantle, triggered by slab break-off following terrane (i.e., arc-continent) collision. This together with other adakitic intrusions are considered to create favourable conditions for orogenic gold mineralization (see Yang and Lawley, 2024a, 2024b), which could be longer lived than what is interpreted by other authors. In the LLGB, three major orogenic Au deposits (Figure GS2024-16-1) are situated nearby adakite-like intrusions (Glendenning et al., 2015; Hastie et al., 2018; Lawley et al., 2020, 2023), suggesting a potential linkage with gold metallogenesis.

In contrast, the 1848.3 ±2.7 Ma leucogranite of the Little Brightsand Lake pluton, which displays a highly evolved geochemical signature, is likely the result of strong fractionation of parental magmas derived from partial melting of crustal materials under relatively reduced redox conditions. A critical factor that needs to be considered in mineral exploration for intrusion-related ore deposits is the current erosion level of the granite intrusions, when investigating and exploring for granitoid intrusion-related mineral deposits (Yang, 2023a). This can be assessed by estimating their emplacement depth and/or crystallization pressure (e.g., Yang, 2017; Yang et al., 2021). More work is required to evaluate potential of granitic pegmatite-hosted rare metals (or critical metals: lithium, tantalum, cesium) mineralization associated with the S-type granodiorite that was identified this past summer in the Zed Lake pluton.

Acknowledgments

The author thanks S. Tetteh providing enthusiastic field assistance, as well as C. Epp and P. Belanger for thorough logistical support and cataloguing and processing of the samples; J. Janssens for assistance in compiling DRI2024011²; and A. Martin, H. Adediran and G. Keller for technical support. C.J.M. Lawley and M.G. Houlé of the Geological Survey of Canada are gratefully acknowledged for their collaborations during the course of this study. M. Hamilton is gratefully acknowledged for providing high quality U-Pb zircon data via an analytical contract with the MGS. The manuscript has benefited greatly from constructive reviews by T. Martins and K. Reid, technical editing by R.F. Davie,

² MGS Data Repository Item DRI2024011, containing the data or other information sources used to compile this report, is available online to download free of charge at <https://manitoba.ca/iem/info/library/downloads/index.html>, or on request from minesinfo@gov.mb.ca, or by contacting the Resource Centre, Manitoba Economic Development, Investment, Trade and Natural Resources, 360-1395 Ellice Avenue, Winnipeg, Manitoba R3G 3P2, Canada.

and report layout by C. Steffano. Alamos Gold Inc. and Corazon Mining Ltd. are gratefully acknowledged for providing various supports.

References

- Anderson, S.D. and Beaumont-Smith, C.J. 2001: Structural analysis of the Pool Lake–Boiley Lake area, Lynn Lake greenstone belt (NTS 64C/11); *in* Report of Activities 2001, Manitoba Industry, Trade and Mines, Manitoba Geological Survey, p. 76–85, URL <<https://manitoba.ca/iem/geo/field/roa01pdfs/01gs-12.pdf>> [November 2019].
- Ansdell, K.M. 2005: Tectonic evolution of the Manitoba-Saskatchewan segment of the Paleoproterozoic Trans-Hudson Orogen, Canada; *Canadian Journal of Earth Sciences*, v. 42, p. 741–759.
- Baldwin, D.A. 1989: Mineral deposits and occurrences in the Lynn Lake area, NTS 64C/14; Manitoba Energy and Mines, Geological Services, Mineral Deposit Series Report No. 6, 130 p., URL <<https://manitoba.ca/iem/info/libmin/MDS6.zip>> [September 2023].
- Baldwin, D.A., Syme, E.C., Zwanzig, H.V., Gordon, T.M., Hunt, P.A. and Stevens, R.P. 1987: U–Pb zircon ages from the Lynn Lake and Rusty Lake metavolcanic belts, Manitoba: two ages of Proterozoic magmatism; *Canadian Journal of Earth Sciences*, v. 24, p. 1053–1063.
- Beaumont-Smith, C.J. 2008: Geochemistry data for the Lynn Lake greenstone belt, Manitoba (NTS 64C11-16); Manitoba Science, Technology, Energy and Mines, Manitoba Geological Survey, Open File OF2007-1, 5 p., URL <<https://manitoba.ca/iem/info/libmin/OF2007-1.zip>> [October 2021].
- Beaumont-Smith, C.J. and Böhm, C.O. 2002: Structural analysis and geochronological studies in the Lynn Lake greenstone belt and its gold-bearing shear zones (NTS 64C10, 11, 12, 14, 15 and 16), Manitoba; *in* Report of Activities 2002, Manitoba Industry, Trade and Mines, Manitoba Geological Survey, p. 159–170, URL <<https://manitoba.ca/iem/geo/field/roa02pdfs/GS-19.pdf>> [October 2021].
- Beaumont-Smith, C.J. and Böhm, C.O. 2003: Tectonic evolution and gold metallogeny of the Lynn Lake greenstone belt, Manitoba (NTS 64C10, 11, 12, 14, 15 and 16), Manitoba; *in* Report of Activities 2003, Manitoba Industry, Economic Development and Mines, Manitoba Geological Survey, p. 39–49, URL <<https://manitoba.ca/iem/geo/field/roa03pdfs/GS-06.pdf>> [October 2021].
- Beaumont-Smith, C.J. and Böhm, C.O. 2004: Structural analysis of the Lynn Lake greenstone belt, Manitoba (NTS 64C10, 11, 12, 14, 15 and 16); *in* Report of Activities 2004, Manitoba Industry, Economic Development and Mines, Manitoba Geological Survey, p. 55–68, URL <<https://manitoba.ca/iem/geo/field/roa04pdfs/GS-06.pdf>> [October 2021].
- Beaumont-Smith, C.J., Machado, N. and Peck, D.C. 2006: New uranium-lead geochronology results from the Lynn Lake greenstone belt, Manitoba (NTS 64C11-16); Manitoba Science, Technology, Energy and Mines, Manitoba Geological Survey, Geoscientific Paper GP2006-1, 11 p., URL <<https://manitoba.ca/iem/info/libmin/GP2006-1.pdf>> [October 2021].
- Bonin, B. 2007: A-type granites and related rocks: evolution of a concept, problems and prospects; *Lithos*, v. 97, p. 1–29.
- Chakhmouradian, A.R., Mumin, A.H., Demény, A. and Elliott, B. 2008: Postorogenic carbonatites at Eden Lake, Trans-Hudson Orogen (northern Manitoba, Canada): geological setting, mineralogy and geochemistry; *Lithos*, v. 103, p. 503–526.
- Chappell, B.W. and White, A.J.R. 1974: Two contrasting granite types; *Pacific Geology*, v. 8, p. 173–174.
- Chappell, B.W. and White, A.J.R. 1992: I- and S-type granites in the Lachlan Fold Belt; *Transactions of the Royal Society of Edinburgh: Earth Sciences*, v. 83, p. 1–26.
- Chappell, B.W. and White, A.J.R. 2001: Two contrasting granite types: 25 years later; *Australian Journal of Earth Sciences*, v. 48, p. 489–499.
- Corfu, F., Hahnchar, J.M., Hoskin, P.W.O. and Kinny, P. 2003: Atlas of zircon textures; *Reviews in Mineralogy and Geochemistry*, v. 53, p. 469–500.
- Corrigan, D. 2012: Paleoproterozoic crustal evolution and tectonic processes: insights from the LITHOPROBE program in the Trans-Hudson orogen, Canada, Chapter 4; *in* Tectonic Styles in Canada: The LITHOPROBE Perspective, J.A. Percival, F.A. Cook and R.M. Clowes (ed.), Geological Association of Canada, Special Paper 49, p. 237–284.
- Corrigan, D., Galley, A.G. and Pehrsson, S. 2007: Tectonic evolution and metallogeny of the southwestern Trans-Hudson Orogen; *in* Mineral Deposits of Canada: A Synthesis of Major Deposit-Types, District Metallogeny, the Evolution of Geological Provinces, and Exploration Methods, W.D. Goodfellow (ed.), Geological Association of Canada, Mineral Deposits Division, Special Publication 5, p. 881–902.
- Corrigan, D., Pehrsson, S., Wodicka, N. and de Kemp, E. 2009: The Palaeoproterozoic Trans-Hudson Orogen: a prototype of modern accretionary processes; *in* Ancient Orogens and Modern Analogues, J.B. Murphy, J.D. Keppie, and A.J. Hynes (ed.), Geological Society of London, Special Publications, v. 327, p. 457–479.
- Eby, G.N. 1990: The A-type granitoids: a review of their occurrence and chemical characteristics and speculations on their petrogenesis; *Lithos*, v. 26, p. 115–134.
- Eby, G.N. 1992: Chemical subdivision of the A-type granitoids: petrogenetic and tectonic implications; *Geology*, v. 20, p. 641–644.
- Fedikow, M.A.F. and Gale, G.H. 1982: Mineral deposit studies in the Lynn Lake area; *in* Report of Field Activities 1982, Manitoba Department of Energy and Mines, Mineral Resources Division, p. 44–54, URL <<https://manitoba.ca/iem/geo/field/rfa1982.pdf>> [October 2022].
- Ferreira, K.J. 1993: Mineral deposits and occurrences in the Laurie Lake area, NTS 64C/12; Manitoba Energy and Mines, Geological Services, Mineral Deposit Series Report No. 9, 101 p., URL <<https://manitoba.ca/iem/info/libmin/MDS9.zip>> [September 2022].
- Frisch, W., Meschede, M. and Blakey, R. 2011: Plate tectonics: Continental drift and mountain building. Springer, Heidelberg, 212 p.
- Gerstenberger, H. and Haase, G. 1997: A highly effective emitter substance for mass spectrometric Pb isotope ratio determinations; *Chemical Geology*, v. 136, p. 309–312.
- Gibson, G.M., Champion, D.C. and Doublier, M.P. 2024: The Paleoproterozoic Trans-Australian Orogen: Its magmatic and tectonothermal record, links to northern Laurentia, and implications for supercontinent assembly; *Geological Society of America Bulletin*, URL <<https://doi.org/10.1130/B36255.1>>.
- Gilbert, H.P. 1993: Geology of the Barrington Lake–Melvin Lake–Fraser Lake area; Manitoba Energy and Mines, Geological Services, Geological Report GR87-3, 97 p., URL <<https://manitoba.ca/iem/info/libmin/GR87-3.zip>> [October 2021].
- Gilbert, H.P., Syme, E.C. and Zwanzig, H.V. 1980: Geology of the metavolcanic and volcanoclastic metasedimentary rocks in the Lynn Lake area; Manitoba Energy and Mines, Mineral Resources Division, Geological Paper GP80-1, 118 p., URL <<https://manitoba.ca/iem/info/libmin/GP80-1.zip>> [October 2021].

- Glendenning, M.W.P., Gagnon, J.E. and Polat, A. 2015: Geochemistry of the metavolcanic rocks in the vicinity of the MacLellan Au-Ag deposit and an evaluation of the tectonic setting of the Lynn Lake greenstone belt, Canada: evidence for a Paleoproterozoic-aged rifted continental margin; *Lithos*, v. 233, p. 46–68.
- Grasso, V.G. 1968: The TiO₂ frequency in volcanic rocks; *Geologische Rundschau*, v. 57, p. 930–935.
- Hamilton, M.A. 2022: Report on U-Pb CA-ID-TIMS geochronology of Archean and Proterozoic rock units in support of Manitoba Geological Survey bedrock mapping programs, 2018–2022; Jack Satterly Geochronology Laboratory, Department of Earth Sciences, University of Toronto, Toronto, Ontario, 51 p.
- Hastie, E.C.G., Gagnon, J.E. and Samson, I.M. 2018: The Paleoproterozoic MacLellan deposit and related Au-Ag occurrences, Lynn Lake greenstone belt, Manitoba: an emerging, structurally controlled gold camp; *Ore Geology Reviews*, v. 94, p. 24–45.
- Hildebrand, R.S., Whalen, J.B. and Bowring, S.A. 2018: Resolving the crustal composition paradox by 3.8 billion years of slab failure magmatism and collisional recycling of continental crust; *Tectonophysics*, v. 734–735, p. 69–88.
- Hoffman, P.H. 1988: United plates of America, the birth of a craton: Early Proterozoic assembly and growth of Laurentia; *Annual Reviews of Earth and Planetary Sciences*, v. 16, p. 543–603.
- Irvine, T.N. and Baragar, W.R.A. 1971: A guide to the chemical classification of the common volcanic rocks; *Canadian Journal of Earth Sciences*, v. 8, p. 523–548.
- Ishihara, S. 1977: The magnetite-series and ilmenite-series granitic rocks; *Mining Geology*, v. 27, p. 293–305, URL <<https://doi.org/10.11456/shigenchishitsu1951.27.293>>.
- Ishihara, S. 1981: The granitoid series and mineralization; *Economic Geology*, 75th Anniversary Volume, p. 458–484, URL <<https://doi.org/10.5382/AV75.14>>.
- Ishihara, S. 2004: The redox state of granitoids relative to tectonic setting and Earth history: the magnetite-ilmenite series 30 years later; *Earth and Environmental Science Transactions of the Royal Society of Edinburgh*, v. 95, p. 23–33, URL <<https://doi.org/10.1017/S0263593300000894>>.
- Jaffey, A.H., Flynn, K.F., Glendenin, L.E., Bentley, W.C. and Essling, A.M. 1971: Precision measurement of half-lives and specific activities of ²³⁵U and ²³⁸U; *Physical Review*, v. 4, p. 1889–1906.
- Jones, L.R., Lafrance, B. and Beaumont-Smith, C.J. 2006: Structural controls on gold mineralization at the Burnt Timber Mine, Lynn Lake Greenstone Belt, Trans-Hudson Orogen, Manitoba; *Exploration and Mining Geology*, v. 15, p. 89–100.
- Krogh, T.E. 1973: A low contamination method for hydrothermal decomposition of zircon and extraction of U and Pb for isotopic age determinations; *Geochimica et Cosmochimica Acta*, v. 37, p. 485–494.
- Lawley, C.J.M., Yang, X.M., Selby, D., Davis, W., Zhang, S., Petts, D.C. and Jackson, S.E. 2020: Sedimentary basin controls on orogenic gold deposits: new constraints from U-Pb detrital zircon and Re-Os sulphide geochronology, Lynn Lake greenstone belt, Canada; *Ore Geology Reviews*, v. 126, art. 103790, URL <<https://doi.org/10.1016/j.oregeorev.2020.103790>>.
- Lawley, C.J.M., Schneider, D.A., Camacho, A., McFarlane, C.R.M., Davis, W.J. and Yang, X.M. 2023: Post-orogenic exhumation triggers gold mobility in the Trans-Hudson orogen: new geochronology results from the Lynn Lake Greenstone Belt, Manitoba, Canada; *Precambrian Research*, v. 395, art. 107127, URL <<https://doi.org/10.1016/j.precamres.2023.107127>>.
- Lewry, J.F. and Collerson, K.D. 1990: The Trans-Hudson Orogen: extent, subdivisions and problems; in *The Early Proterozoic Trans-Hudson Orogen of North America*, J.F. Lewry and M.R. Stauffer (ed.), Geological Association of Canada, Special Paper 37, p. 1–14.
- Lin, S. and Beakhouse, G.P. 2013: Synchronous vertical and horizontal tectonism at late stages of Archean cratonization and genesis of Hemlo gold deposit, Superior craton, Ontario, Canada; *Geology*, v. 41, p. 359–362.
- Ludwig, K.R. 2009: User's manual for Isoplot 3.71 a geochronological toolkit for Excel; Berkeley Geochronological Center Special Publication 4, 72 p.
- Maniar, P.D. and Piccoli, P.M. 1989: Tectonic discrimination of granitoids; *Geological Society of America Bulletin*, v. 101, p. 635–643.
- Manitoba Agriculture and Resource Development 2021: Lynn Lake, Manitoba (NTS 64C14); Manitoba Agriculture and Resource Development, Manitoba Geological Survey, Lynn Lake Bedrock Compilation Map 64C14, scale 1:50 000, URL <https://manitoba.ca/iem/info/libmin/lynn_lake_compilation_2021.zip> [October 2021].
- Manitoba Energy and Mines 1986: Granville Lake, NTS 64C; Manitoba Energy and Mines, Minerals Division, Bedrock Geology Compilation Map 64C, scale 1:250 000, URL <https://manitoba.ca/iem/info/libmin/bgcms/bgcms_granville_lake.pdf> [October 2022].
- Martin, H., Smithies, R.H., Rapp, R., Moyen, J.-F. and Champion, D. 2005: An overview of adakite, tonalite–trondhjemite–granodiorite (TTG), and sanukitoid: relationships and some implications for crustal evolution; *Lithos*, v. 79, p. 1–24.
- Martin, H., Moyen, J.-F. and Rapp, R. 2009: The sanukitoid series: magmatism at the Archean-Proterozoic transition; *Earth and Environmental Science Transactions of The Royal Society of Edinburgh*, v. 100, Special Issue 1-2, p. 15–33.
- Martins, T., Rayner, N., Corrigan, D. and Kremer, P. 2022: Regional geology and tectonic framework of the Southern Indian domain, Trans-Hudson orogen, Manitoba; *Canadian Journal of Earth Sciences*, v. 59, p. 371–388, URL <<https://doi.org/10.1139/cjes-2020-0142>>.
- Mattinson, J. 2005: Zircon U-Pb chemical abrasion (CA-TIMS) method: Combined annealing and multi-step partial dissolution analysis for improved precision and accuracy of zircon ages; *Chemical Geology*, v. 220, p. 47–66.
- Middlemost, E.A.K. 1994: Naming materials in the magma/igneous rock system; *Earth-Science Reviews*, v. 37, p. 215–224.
- Milligan, G.C. 1960: Geology of the Lynn Lake district; Manitoba Department of Mines and Natural Resources, Mines Branch, Publication 57-1, 317 p.
- Mumin, A.H. 2002: Discovery of a carbonatite complex at Eden Lake (NTS 64C9), Manitoba; in *Report of Activities 2002*, Manitoba Industry, Trade and Mines, Manitoba Geological Survey, p. 187–197, URL <<https://manitoba.ca/iem/geo/field/roa02pdfs/GS-21.pdf>> [August 2024].
- Richards, J.P. and Kerrich, R. 2007: Special paper: Adakite-like rocks: their diverse origins and questionable role in metallogenesis; *Economic Geology*, v. 102, p. 537–576.
- Rittmann, A. 1962: *Volcanoes and their activity*; Wiley, New York, USA, 305 p.
- Rittmann, A. 1973: *Stable mineral assemblages of igneous rocks*; Springer-Verlag, Berlin, Germany, 262 p.
- Rubatto, D. 2017: Zircon: the metamorphic mineral; *Reviews in Mineralogy & Geochemistry*, v. 83, p. 297–328.

- Shirey, S.B. and Hanson, G.N. 1984: Mantle derived Archaean monzodiorites and trachyandesites; *Nature*, v. 310, p. 222–224.
- Stacey, J.S. and Kramers, J.D. 1975: Approximation of terrestrial lead isotope evolution by a two-stage model; *Earth and Planetary Science Letters*, v. 26, p. 207–221.
- Sun, W.D., Ling, M.X., Yang, X.Y., Fan, W.M., Ding, X. and Liang, H.Y. 2010: Ridge subduction and porphyry copper-gold mineralization: an overview; *Science China Earth Sciences*, v. 53, p. 475–484.
- Syme, E.C. 1985: Geochemistry of metavolcanic rocks in the Lynn Lake Belt; Manitoba Energy and Mines, Geological Services, Geological Report GR84-1, 84 p., 1 map, 1:100 000 scale.
- Turek, A., Woodhead, J. and Zwanzig H.V. 2000: U-Pb age of the gabbro and other plutons at Lynn Lake (part of NTS 64C); *in* Report of Activities 2000, Manitoba Industry, Trade and Mines, Manitoba Geological Survey, p. 97–104, URL <<https://manitoba.ca/iem/geo/field/roa00pdfs/00gs-18.pdf>> [October 2021].
- Whalen, J.B. and Hildebrand, R.S. 2019: Trace element discrimination of arc, slab failure, and A-type granitic rocks; *Lithos*, v. 348–349, art. 105179.
- Whalen, J.B., Currie, K.L. and Chappell, B.W. 1987: A-type granites: geochemical characteristics, discrimination and petrogenesis; *Contributions to Mineralogy and Petrology*, v. 95, p. 407–419.
- White, D.J., Zwanzig, H.V. and Hajnal, Z. 2000: Crustal suture preserved in the Paleoproterozoic Trans-Hudson orogeny, Canada; *Geology*, v. 28, p. 527–530.
- Yang, X.M. 2007: Using the Rittmann Serial Index to define the alkalinity of igneous rocks; *Neues Jahrbuch für Mineralogie*, v. 184, p. 95–103.
- Yang, X.M. 2017: Estimation of crystallization pressure of granite intrusions; *Lithos*, v. 286–287, p. 324–329, URL <<https://doi.org/10.1016/j.lithos.2017.06.018>>.
- Yang, X.M. 2019: Preliminary results of bedrock mapping in the Gemmell Lake area, Lynn Lake greenstone belt, northwestern Manitoba (parts of NTS 64C11, 14); *in* Report of Activities 2019, Manitoba Agriculture and Resource Development, Manitoba Geological Survey, p. 10–29, URL <<https://manitoba.ca/iem/geo/field/roa19pdfs/GS2019-2.pdf>> [October 2021].
- Yang, X.M. 2020: Bedrock geochemical data of the Gemmell Lake area, Lynn Lake greenstone belt, northwestern Manitoba (parts of NTS 64C11, 14); Manitoba Agriculture and Resource Development, Manitoba Geological Survey, Data Repository Item DRI2020009, Microsoft® Excel® file.
- Yang, X.M. 2021a: Bedrock mapping at Ralph Lake, Lynn Lake greenstone belt, northwestern Manitoba (part of NTS 64C14): preliminary results and geological implications; *in* Report of Activities 2021, Manitoba Agriculture and Resource Development, Manitoba Geological Survey, p. 40–58, URL <<https://manitoba.ca/iem/geo/field/roa21pdfs/GS2021-5.pdf>> [November 2021].
- Yang, X.M. 2021b: Bedrock geochemical data of the Ralph Lake area, Lynn Lake greenstone belt, northwestern Manitoba (parts of NTS 64C14); Manitoba Agriculture and Resource Development, Manitoba Geological Survey, Data Repository Item DRI2021021, Microsoft® Excel® file.
- Yang, X.M. 2022: Preliminary results of bedrock geological mapping in the Fox mine–Snake Lake area, Lynn Lake greenstone belt, northwestern Manitoba (part of NTS 64C12); *in* Report of Activities 2022, Manitoba Natural Resources and Northern Development, Manitoba Geological Survey, p. 71–86, URL <<https://manitoba.ca/iem/geo/field/roa22pdfs/GS2022-9.pdf>> [November 2022].
- Yang, X.M. 2023a: Progress report on the study of granitoids in Manitoba: petrogenesis and metallogeny; Manitoba Economic Development, Investment and Trade, Manitoba Geological Survey, Open File OF2022-3, 119 p., URL <<https://manitoba.ca/iem/info/libmin/OF2022-3.zip>> [March 2023].
- Yang, X.M. 2023b: Field relationships, geochemical characteristics and metallogenic implications of gabbroic intrusions in the Paleoproterozoic Lynn Lake greenstone belt, northwestern Manitoba (parts of NTS 64C10–12, 14–16); *in* Report of Activities 2023, Manitoba Economic Development, Investment, Trade and Natural Resources, Manitoba Geological Survey, p. 73–89, URL <<https://manitoba.ca/iem/geo/field/roa23pdfs/GS2023-9.pdf>> [November 2023].
- Yang, X.M. 2024: Geochemical data of bulk-rock samples collected in the 2022 and 2023 field seasons from the Lynn Lake greenstone belt, northwestern Manitoba (parts of NTS 64C10–12, 14–16); Manitoba Economic Development, Investment, Trade and Natural Resources, Manitoba Geological Survey, Data Repository Item DRI2024011, Microsoft® Excel® file.
- Yang, X.M. and Beaumont-Smith, C.J. 2015: Granitoid rocks in the Lynn Lake region, northwestern Manitoba: preliminary results of reconnaissance mapping and sampling; *in* Report of Activities 2015, Manitoba Mineral Resources, Manitoba Geological Survey, p. 68–78, URL <<https://manitoba.ca/iem/geo/field/roa15pdfs/GS-5.pdf>> [October 2021].
- Yang, X.M. and Beaumont-Smith, C.J. 2016: Geological investigations in the Farley Lake area, Lynn Lake greenstone belt, northwestern Manitoba (part of NTS 64C16); *in* Report of Activities 2016, Manitoba Growth, Enterprise and Trade, Manitoba Geological Survey, p. 99–114, URL <<https://manitoba.ca/iem/geo/field/roa16pdfs/GS-9.pdf>> [October 2021].
- Yang, X.M. and Beaumont-Smith, C.J. 2017: Geological investigations of the Wasekwan Lake area, Lynn Lake greenstone belt, northwestern Manitoba (parts of NTS 64C10, 15); *in* Report of Activities 2017, Manitoba Growth, Enterprise and Trade, Manitoba Geological Survey, p. 117–132, URL <<https://manitoba.ca/iem/geo/field/roa17pdfs/GS2017-11.pdf>> [October 2021].
- Yang, X.M. and Lawley, C.J.M. 2018: Tectonic setting of the Gordon gold deposit, Lynn Lake greenstone belt, northwestern Manitoba (parts of NTS 64C16): evidence from litho-geochemistry, Nd isotopes and U-Pb geochronology; *in* Report of Activities 2018, Manitoba Growth, Enterprise and Trade, Manitoba Geological Survey, p. 89–109, URL <<https://manitoba.ca/iem/geo/field/roa18pdfs/GS2018-8.pdf>> [October 2021].
- Yang, X.M. and Lawley, C.J.M. 2024a: Rapid switch in geodynamic setting revealed by episodic granitoid magmatism in the Lynn Lake greenstone belt of Paleoproterozoic Trans-Hudson Orogen, Manitoba, Canada; *Lithos*, v. 470–471, art. 107534, URL <<https://doi.org/10.1016/j.lithos.2024.107534>>.
- Yang, X.M. and Lawley, C.J.M. 2024b: Adakite-like granitoid intrusions in the Paleoproterozoic Lynn Lake greenstone belt, northwestern Manitoba, Canada: Implications for geodynamic setting and gold mineralization [abstract]; Geological Association of Canada–Mineralogical Association of Canada and the 10th International Symposium on granitic pegmatites, Joint Annual Meeting, Brandon, Manitoba, May 19–22, 2024, Program with Abstracts; *Geoscience Canada*, v. 51, p. 127, URL <<https://doi.org/10.12789/geocanj.2024.51.211>>.
- Yang, X.M., Drayson, D. and Polat, A. 2019: S-type granites in the western Superior Province: a marker of Archean collision zones; *Canadian Journal of Earth Sciences*, v. 56, p. 1409–1436, URL <<https://doi.org/10.1139/cjes-2018-0056>>.

- Yang, X.M., Lentz, D.R. and Chi, G. 2021: Ferric-ferrous iron oxide ratios: Effect on crystallization pressure of granites estimated by Qtz-geobarometry; *Lithos*, v. 380-381, art. 105920, URL <<https://doi.org/10.1016/j.lithos.2020.105920>>.
- Yousefi, F. and Lentz D.R. 2024: Formation of high-silica adakites and their relationship with slab break-off: implications for generating fertile Cu-Au-Mo porphyry systems; *Geoscience Frontiers*, v. 15, art. 101927, URL <<https://doi.org/10.1016/j.gsf.2024.101927>>.
- Zwanzig, H.V. 2000: Geochemistry and tectonic framework of the Kisseynew Domain–Lynn Lake belt boundary (part of NTS 63P/13); *in* Report of Activities 2000, Manitoba Industry, Trade and Mines, Manitoba Geological Survey, p. 91–96, URL <<https://manitoba.ca/iem/geo/field/roa00pdfs/00gs-17.pdf>> [October 2021].
- Zwanzig, H. 2024: Tectonic model of the Paleoproterozoic western Trans-Hudson Orogen [abstract]; Geological Association of Canada–Mineralogical Association of Canada and the 10th International Symposium on granitic pegmatites, Joint Annual Meeting, Brandon, Manitoba, May 19–22, 2024, Program with Abstracts; *Geoscience Canada*, v. 51, p. 128, URL <<https://doi.org/10.12789/geocanj.2024.51.211>>.
- Zwanzig, H.V. and Bailes, A.H. 2010: Geology and geochemical evolution of the northern Flin Flon and southern Kisseynew domains, Kisseynew–File lakes area, Manitoba (parts of NTS 63K, N); Manitoba Innovation, Energy and Mines, Manitoba Geological Survey, Geoscientific Report GR2010-1, 135 p., URL <<https://manitoba.ca/iem/info/libmin/GR2010-1.zip>> [October 2021].
- Zwanzig, H.V., Syme, E.C. and Gilbert, H.P. 1999: Updated trace element geochemistry of the ca. 1.9 Ga metavolcanic rocks in the Paleoproterozoic Lynn Lake belt; Manitoba Industry, Trade and Mines, Geological Services, Open File Report OF99-13, 46 p., URL <<https://manitoba.ca/iem/info/libmin/OF99-13.zip>> [October 2020].